

Spontaneous magnetic moments in $\text{YBa}_2\text{Cu}_3\text{O}_{7-\delta}$ thin films

F. Tafuri

*Dip. di Ingegneria dell'Informazione, Seconda Università di Napoli, Aversa (CE) and
INFN - Dip. di Scienze Fisiche, Università di Napoli Federico II, Napoli, Italy*

J.R. Kirtley

IBM T.J. Watson Research Center, P.O. Box 218, Yorktown Heights, NY 10598, USA

(February 1, 2008)

We have observed spontaneous magnetic moments with random signs in c -axis oriented thin films of the high- T_c cuprate superconductor $\text{YBa}_2\text{Cu}_3\text{O}_{7-\delta}$ (YBCO), imaged with a scanning SQUID microscope. These moments arise when the samples become superconducting, and appear to be associated with non-ferromagnetic defects in the films. In contrast with granular high- T_c samples, which also show spontaneous moments with random signs, the present samples shield diamagnetically.

It now appears likely that the superconductivity in optimally doped cuprate high- T_c superconductors can be characterized by an orbital component of the pairing wavefunction with predominantly $d_{x^2-y^2}$ symmetry [1–3]. The $d_{x^2-y^2}$ order parameter does not violate time reversal symmetry [4,5], and little, if any, time reversal symmetry breaking is observed experimentally in the bulk material [6]. Nevertheless, it has been shown theoretically that broken time-reversal symmetry (BTRS) could occur locally in a $d_{x^2-y^2}$ superconductor at certain surfaces and interfaces, or in the presence of non-magnetic and magnetic impurities [7–11]. The existence of a lowest energy state which is not unique (BTRS) requires an additional component of the order parameter that is $\pi/2$ out of phase with the $d_{x^2-y^2}$ component. A $d_{x^2-y^2} + is$ or $d_{x^2-y^2} + id_{xy}$ pairing state has been suggested near a surface or twin boundary with (110) orientation, producing a local nodeless global gap function [10–12]. The predicted BTRS should manifest itself in many effects, including deviations from the well-established Josephson's sinusoidal current-phase relationship [13], and the splitting of the zero bias conductance peak induced by the Andreev surface bound states [14]. An intrinsic phase shift in Josephson junctions is a signature of BTRS associated with a grain boundary or a barrier interface and should produce spontaneous supercurrents, possible fractional flux quanta and phase slips [4].

However, experimental measurements using scanning SQUID microscopy have shown no evidence for BTRS in YBCO tricrystal samples [15,16], in YBCO-Pb thin-film SQUIDs [17], or in sparsely twinned YBCO single crystals [18]. These samples each have some combination of grain boundaries, tunnel junctions, and twin boundaries, which might be expected to induce $d_{x^2-y^2} + is$ or $d_{x^2-y^2} + id_{xy}$ local pairing in a bulk $d_{x^2-y^2}$ superconductor. On the other hand, measurements of the magnetic field dependence of the zero-bias anomaly in thin film YBCO/I/Cu tunnel junctions [14], and a spontaneous net magnetic moment in bulk SQUID magnetization measurements of c -axis YBCO thin films [19],

support BTRS. We note that in these last two experiments, evidence for broken time-reversal symmetry was not seen in all samples. In this paper we provide experimental evidence for large spontaneous flux generation in YBCO c -axis oriented thin films, apparently associated with non-ferromagnetic defects in the films. Such spontaneous moments could result in the effects reported in support of BTRS previously [14,19]. We speculate on the source of our observed magnetic moments.

Our measurements were made on biepitaxial 45° a -axis tilt (twist) grain boundary Josephson junctions (GBJs) employing films with different orientations [20] (Fig. 1(a) is, for example, the schematic of a tilt GBJ imaged in Fig. 1(b)). Details on the scanning SQUID measurements can be found elsewhere [21]. Our samples employed a (110) MgO film as a seed layer to modify the crystal orientation of YBCO on the (110) SrTiO_3 substrate. YBCO grows predominantly along the [103] or [013] directions on the SrTiO_3 substrate, and along the [001] direction on the MgO seed layer. These structures allow us to investigate regions with different properties and morphologies simultaneously. Details of the fabrication process of the junctions have been described elsewhere, along with a complete characterization of the microstructure and transport properties [20]. These films are affected by the presence of Y-based impurities, as is commonly observed in YBCO thin films deposited by sputtering [22]. Y_2O_3 and Y_2BaCuO_5 (Y211) precipitates are in general found in the (103) and (001) electrodes, as shown by transmission electron microscopy (TEM) analyses [20,22]. The amount of the precipitates can be modified and very roughly controlled by changing the YBCO deposition conditions. The presence of Y211 precipitates can be revealed by Scanning Electron Microscopy (SEM) or Atomic Force Microscopy (AFM) with some accuracy. TEM analysis shows that there are no grain boundaries in the (001) films [20,22].

The spatial distribution of the magnetic flux for a (001)/(103) 45° twist biepitaxial grain boundary sample is shown in Fig. 1(b). The sample was cooled in a field of ~ 5 mG and imaged at 4.2K with an octagonal shaped

low- T_c SQUID sensor pickup loop 4 microns in diameter. In this image the (103) YBCO film is magnetically smooth, aside from a single dipole feature (often seen in YBCO films), and 4 vortices trapped in the bulk of the film. The vortices in the (103) film are anisotropic, elongated in the a-b plane direction. In contrast, the (001) YBCO on the MgO seed layer has many localized regions of flux, with the fields pointing both out of (white) and into (black) the sample. When the sample is cooled in zero field, the (103) section has no vortices, but the (001) section still shows many localized magnetic moments, averaging to zero net magnetization. The (001) region is so magnetically disordered that vortices are not well separated, and therefore estimates of the total flux in each “vortex” are difficult. Nevertheless, modelling of the most isolated regions of flux give values for the total flux significantly less than the superconducting flux quantum. An example is shown in Fig. 1(c), which shows experimental data and modelling for a cross-section through Fig. 1(b) as indicated by the nearly horizontal dotted line. This cross-section passes directly through two vortices on opposite sides of the grain boundary (indicated by the nearly vertical dashed line). We model the vortices in the (103) region as anisotropic vortices emerging normal to a surface and parallel to the planes of a layered superconductor. The z -component of such a superconducting vortex is given by [23]:

$$h_z(\mathbf{r}, z) = - \int \frac{d^2\mathbf{k}}{(2\pi)^2} k\phi(\mathbf{k})e^{i\mathbf{k}\cdot\mathbf{r}-kz}, \quad (1)$$

where

$$\phi(\mathbf{k}) = - \frac{\phi_0(1 + m_1 k_x^2)}{m_3 \alpha_3 [m_1 k_x^2 \alpha_3 (k + \alpha_1) + k \alpha_3 + k_y^2]}, \quad (2)$$

$\alpha_1 = ((1 + m_1 k^2)/m_1)^{1/2}$, $\alpha_3 = ((1 + m_1 k_x^2 + m_3 k_y^2)/m_3)^{1/2}$, $k = (k_x^2 + k_y^2)^{1/2}$, $m_1 = \lambda_{ab}^2/\lambda^2$, $m_3 = \lambda_c^2/\lambda^2$, $\lambda = (\lambda_{ab}^2 \lambda_c)^{1/3}$, λ_{ab} is the in-plane penetration depth, $\phi_0 = hc/2e$ is the superconducting flux quantum, h is Planck’s constant, e is the charge on the electron, x is the distance perpendicular to the planes, and y is the distance parallel to the planes. The z -component of the field is integrated over the known geometry of the pickup loop to obtain a flux to compare with experiment. The solid line through the vortex to the right of Fig. 1(c) is a fit of Eq. 1 to the experiment (dots) with the height $z=2.45\mu\text{m}$ of the pickup loop and the c -axis penetration depth $\lambda_c=5.9\mu\text{m}$ as the two fitting parameters, with $\lambda_{ab}=0.14\mu\text{m}$ held fixed. For comparison, the solid line to the left of Fig. 1(c) is the expected flux through the pickup loop for a monopole vortex field source with ϕ_0 total flux, $B_z=(\phi_0/2\pi)z/|r|^3$, using $z=2.45\mu\text{m}$ from the fit to the vortex in the (103) film. The “vortex” in the (001) film is resolution limited using our $4\mu\text{m}$ SQUID pickup loop, but apparently has less than ϕ_0 of flux. The

dashed curve is the prediction for a monopole source with $0.4\phi_0$ total flux.

The source of the spontaneous moments in the c -axis YBCO electrode is not known. To our knowledge this is the first time they have been magnetically imaged in c -axis YBCO. Since there are no grain boundaries in the (001) films, the magnetic roughness must be related to some other aspect of the morphology of the sample. We speculate that it is due to the presence of defects in the film. Figure 2 shows a comparison of SSM and scanning electron microscope (SEM) images of the same region of c -axis film. There appears to be some correlation between defects seen in the SEM images and the magnetic structure. The ovals in Figure 2 are intended as guides to the eye of some of these correlations. Since the predominant defects in these films are Y211 precipitates, we speculate that these are causing the spontaneous magnetization in these films. Y211 is insulating, with an antiferromagnetic ordering temperature between 15 and 30K [24–26]

Figure 3 shows a series of scanning SQUID microscope images of one of our samples for selected temperatures [27]. In these images the sample was cooled in nominal zero field, and then imaged while warming with a square pickup loop $17.8\mu\text{m}$ on a side. The individual “fractional” vortices are not resolved with this larger pickup loop, as they were using the $4\mu\text{m}$ pickup loop. As the critical temperature ($\sim 80\text{K}$ for this film) is approached, “telegraph noise” develops in the images, presumably due to reversals in the sign of the flux generated at particular sites. This “telegraph noise” appears to be driven by interactions with the SQUID pickup loop, as evidenced by the streaking of the images, in the (vertical) scan direction. The total variation in flux decreases as T_c is approached, until above T_c the only magnetic signals present are a few dipoles, presumably due to ferromagnetic particles in the sample. These residual features are square, reflecting the shape of the pickup loop. These images demonstrate that the spontaneous magnetization seen in these samples is intimately related to the superconductivity, and that the defects seen in these films are only weakly, if at all, ferromagnetic above the superconducting critical temperature.

The spontaneous magnetization in these samples is qualitatively similar to that seen [28] in granular BSCCO samples which show the paramagnetic Meissner (Wohllleben) effect, both in terms of its absolute magnitude and its random orientation. However, there is an important difference: these films show diamagnetic shielding at fields of a few milliGauss. An example is shown in Fig. 4. Fig. 4a is a scanning SQUID microscope image of a sample cooled in an externally applied field of 2.5mG , using a $17.8\mu\text{m}$ square pickup loop, and imaged in the same field at a sample temperature of 60K . Also shown are histograms of the relative frequency of flux observed in the upper (001) section of the YBCO film (Fig. 4(b)), and the lower (103) YBCO (Fig. 4(c)).

These histograms show that although the measured flux above the (001) section has a large distribution width, it has the same average flux as above the (103) section. Both show diamagnetic shielding on average. In contrast, granular BSCCO samples show paramagnetic shielding when cooled in fields below about 0.5G [28,29].

Our measurements show that spontaneously generated moments can occur in samples of high- T_c superconductors which do not have π -loops in the presence of grain boundaries. One explanation for these observations is the existence of an out-of-phase component to the dominant $d_{x^2-y^2}$ superconducting order parameter, as predicted in the presence of interfaces or impurities [7]. Since such a complex order parameter would break time-reversal symmetry, this interpretation is consistent with the presence of “vortices” which appear to have less than the superconducting quantum of flux. An alternate explanation [30] is the pinning of a vortex tangle, produced near T_c in a Kosterlitz-Thouless [31] type transition in the nearly two dimensional superconductor YBCO. This pinning would be facilitated by the disorder present in these films. This explanation seems inconsistent with the temperature dependent measurements (Fig. 3), which show more pronounced magnetic structure as T is reduced. However, it could be argued that the vortex-antivortex fluctuations are too rapid close to T_c to be imaged with the SSM. Our measurements are consistent with the absence of effects associated with time-reversal symmetry breaking in most measurements, and the appearance of such effects, which may be associated with small concentrations of defects, in others. Our experiments raise the possibility of intentionally introducing time-reversal symmetry breaking effects by, for example, photolithographically patterning small defects in high- T_c samples. This could be applicable to (e.g.) the fabrication of elements for quantum computation [32], opening new perspectives in the design of such devices without necessarily using Josephson junctions. Possible advantages may be also related to the smaller values of the magnetic flux associated with “fractional vortices”.

We would like to thank J.R. Clem, V.G. Kogan, K.A. Moler and C.C. Tsuei for useful discussions, M.B. Ketchen for the design, and M. Bhushan for the fabrication of the SQUIDS used in this study, and F. Carillo, E. Sarnelli and G. Testa for some help in the preparation of the junctions. F.T. has been partially supported by the projects PRA-INFM “HTS Devices” and by a MURST COFIN98 program (Italy).

Physical Properties of High Temperature Superconductors V, edited by D.M. Ginsberg (World Scientific, Singapore, 1996) Chapter 6, p. 376.

- [3] C.C. Tsuei and J.R. Kirtley, Rev. Mod. Physics, to be published.
- [4] D.B. Bailey, M. Sigrist, and R.B. Laughlin, Phys. Rev. B **55**, 15239 (1997).
- [5] M. Sigrist, Progr. Theor. Physics **99**, 899 (1998).
- [6] S. Spielman *et al.* Phys. Rev. Lett. **68**, 3472 (1992).
- [7] M. Matsumoto and H. Shiba, J. Phys. Soc. Jpn. **64**, 1703; *ibid.*, 3384; *ibid.*, 4867.
- [8] A.B. Kuklov and M. Sigrist, Int. J. Modern. Physics B **11**, 1113 (1997); A.B. Kuklov Phys. Rev. B **52**, R7002 (1995).
- [9] M.E. Simon and C.M. Varma, Phys. Rev. B **60**, 9744 (1999).
- [10] A.V. Balatsky, Phys. Rev. Lett. **80**, 1972 (1998).
- [11] J.-X. Zhu and C.S. Ting, Phys. Rev. B **60**, R 3739 (1999).
- [12] M.I. Salkola and J.R. Schrieffer, Phys. Rev. B **58**, R5952 (1998).
- [13] E. Il'ichev, V. Zakosarenko, R.P.J. IJsselstein, V. Schultze, H.-G. Meyer, H.E. Hoenig, H. Hilgenkamp, and J. Mannhart, Phys. Rev. Lett. **81**, 894 (1998).
- [14] M. Covington, M. Aprili, E. Paraoanu, L.H. Greene, F. Xu, J. Zhu, and C.A. Mirkin, Phys. Rev. Lett. **79**, 277 (1997).
- [15] J.R. Kirtley *et al.* Nature (London) **373**, 225 (1995).
- [16] J.R. Kirtley, C.C. Tsuei, and K.A. Moler, Science **285**, 1373 (1999).
- [17] A. Mathai *et al.* Phys. Rev. Lett. **74**, 4523 (1995).
- [18] K.A. Moler, J.R. Kirtley, R. Liang, D.A. Bonn, and W.N. Hardy, Phys. Rev. B **55**, 12753 (1997).
- [19] R. Carmi, E. Polturak, G. Koren, and A. Auerbach, Cond. Mat. 0001050 (2000).
- [20] F. Tafuri, F. Miletto Granozio, F. Carillo, A. Di Chiara, K. Verbist, and G. Van Tendeloo, Phys. Rev. B **59**, 11523 (1999).
- [21] J.R. Kirtley *et al.* Appl. Phys. Lett. **66**, 1138 (1995).
- [22] U. Scotti di Uccio, F. Miletto Granozio, A. Di Chiara, F. Tafuri, O. Lebedev, K. Verbist, G. Van Tendeloo, Physica C **321**, 162 (1999).
- [23] J.R. Kirtley, V.G. Kogan, J.R. Clem, and K.A. Moler, Phys. Rev. B **59** 4343 (1999). The model used here is for vortices oriented parallel to, and emerging from a surface normal to, the planes. The (103) film surfaces are at a 45° angle to the planes, so this model is not strictly applicable, and the value for λ_c reported here is only approximate.
- [24] A. Weidinger *et al.*, Physica C **153-155**, 168 (1988).
- [25] T. Chattopadhyay, P.J. Brown, U. Könler, and M. Wilhelm, Europhys. Lett. **8**, 685 (1989).
- [26] C. Meyer *et al.*, Solid State Commun. **74**, 1339 (1990).
- [27] J.R. Kirtley, C.C. Tsuei, K.A. Moler, V.G. Kogan, J.R. Clem, and A.J. Turberfield, Appl. Phys. Lett. **74**, 4011 (1999).
- [28] J.R. Kirtley, A.C. Mota, M. Sigrist, and T.M. Rice, J. Phys. Condens. Matter. **10**, L97-103 (1998).
- [29] M. Sigrist and T.M. Rice, Rev. Mod. Phys. **67**, 503 (1995).
- [30] We would like to thank J.R. Clem and V.G. Kogan for suggesting this possibility to us.

[1] D.J. Scalapino, Physics Reports **250**, 329 (1995).

[2] J.F. Annett, N.D. Goldenfeld, and A.J. Leggett, in

- [31] J.M. Kosterlitz and D.J. Thouless, *J. Phys. C* **6**, 1181 (1973).
- [32] L.B. Ioffe, V.B. Geshkenbein, M.V. Feigel'man, A.L. Fauchere, and G. Blatter, *Nature (London)* **398**, 679 (1999); G. Blatter, V. B. Geshkenbein and L. B. Ioffe, *Cond. Mat.* 9912163 (1999).

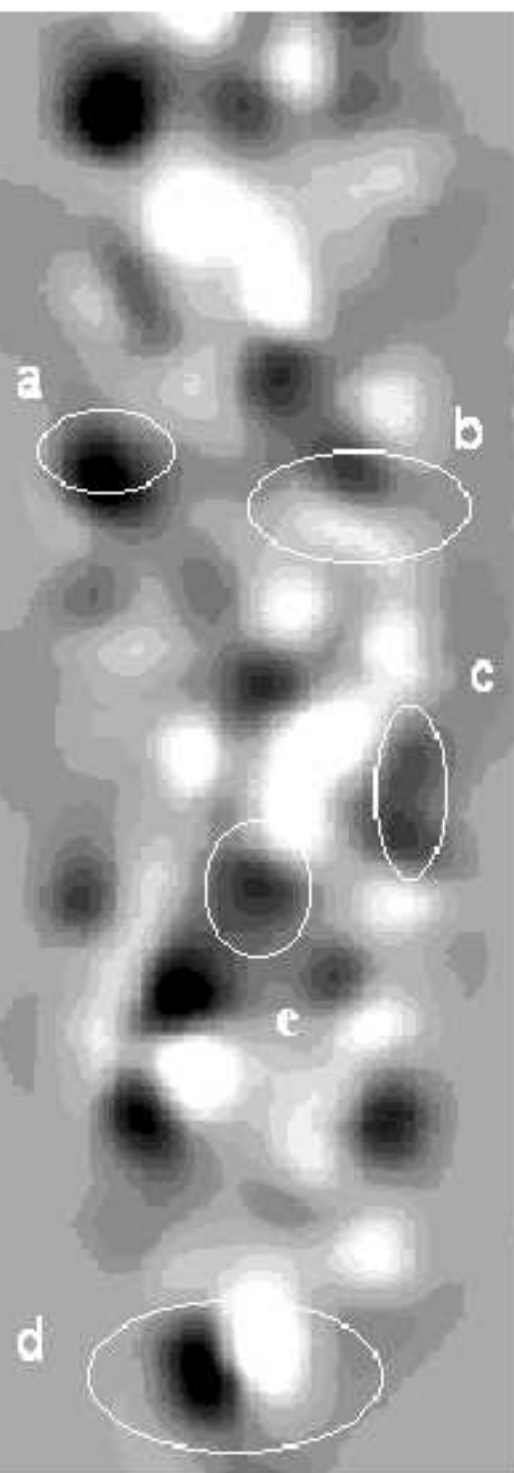
FIG. 1. (a) Schematic of the geometry of a (001)/(103) biepitaxial YBCO grain boundary sample. (b) Scanning SQUID microscope image of such a grain boundary, cooled in ~ 5 mG field and imaged at 4.2K with an octagonal pickup loop $4\mu\text{m}$ in diameter. The grain boundary, indicated by a dashed line, runs nearly vertically through the center of the image. (c) The dots are a cross-section through the image (b) as indicated by the nearly horizontal dotted line, through a “vortex” on either side of the grain boundary. The lines are fits to the data as described in the text.

FIG. 2. Comparison between scanning SQUID microscope (SSM) and scanning electron microscope (SEM) images of the same area of a (001) YBCO thin film. The labelled regions are guides to the eye for areas of correlation between the images.

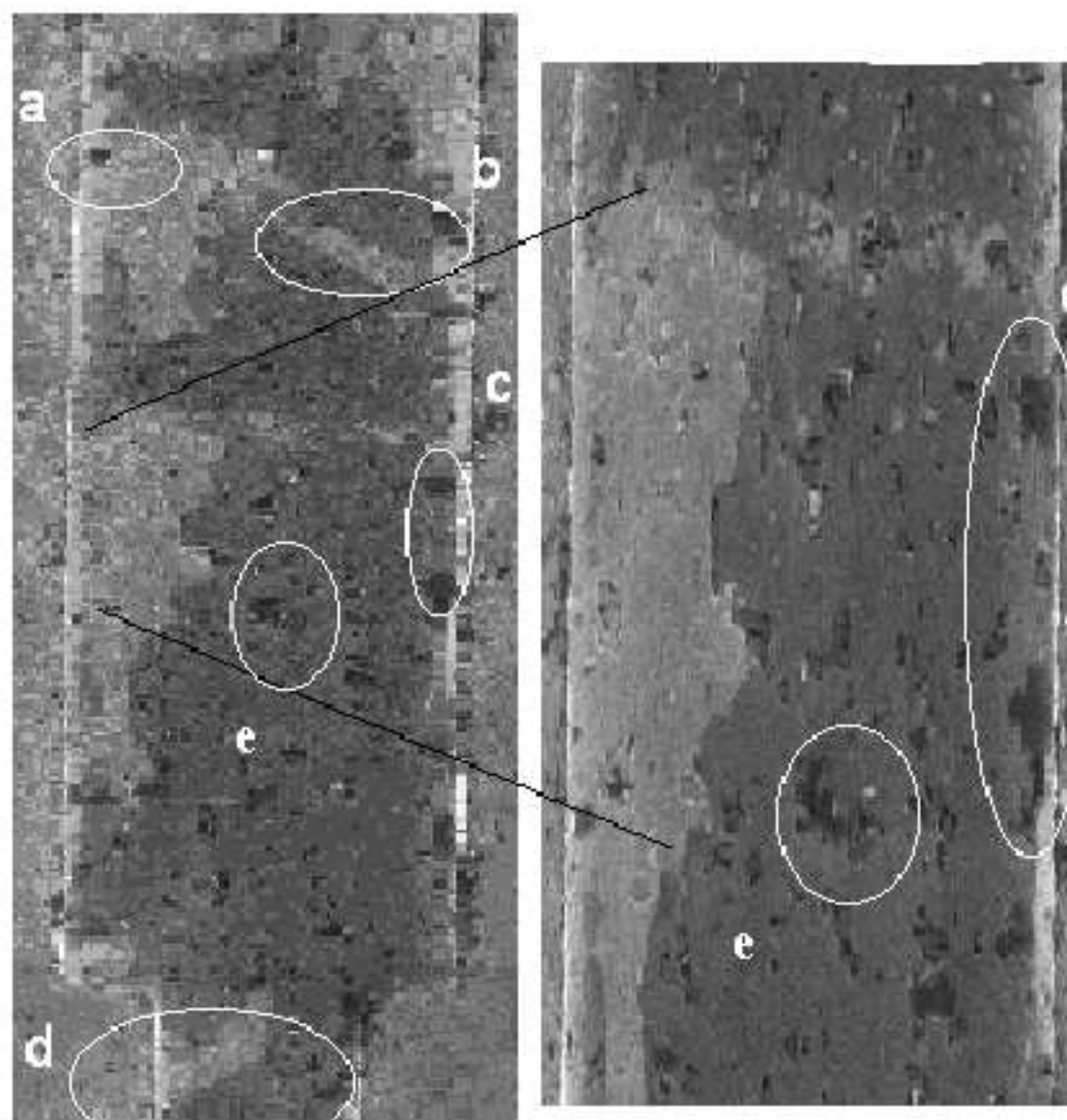
FIG. 3. Scanning SQUID microscope images of a (001)/(103) biepitaxial SQUID, cooled in zero field, and imaged with a $17.8\mu\text{m}$ diameter square pickup loop, for selected temperatures.

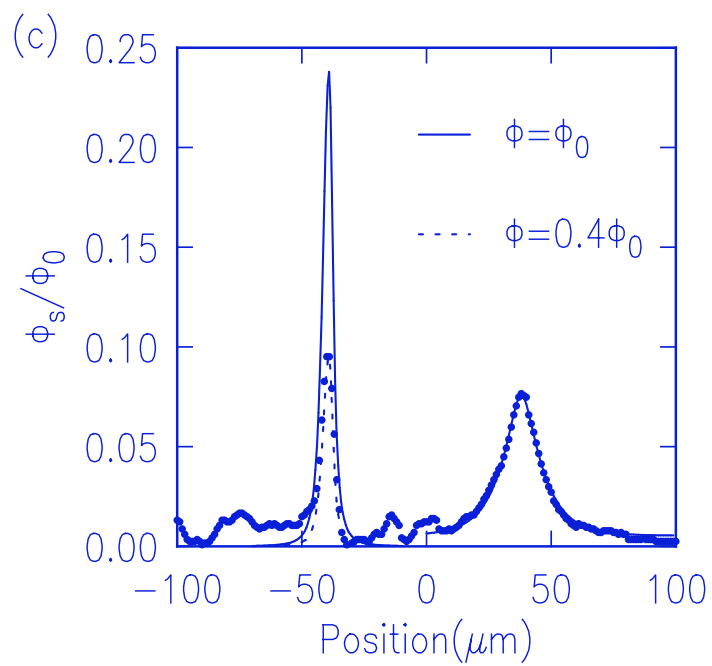
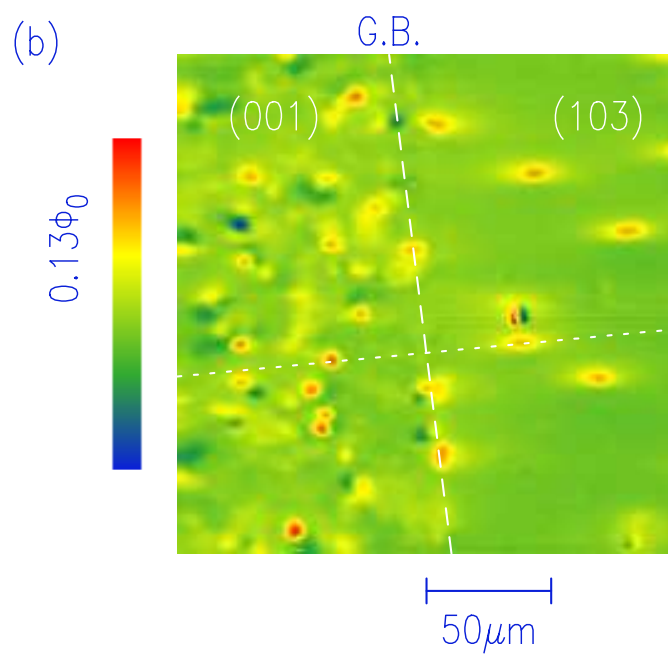
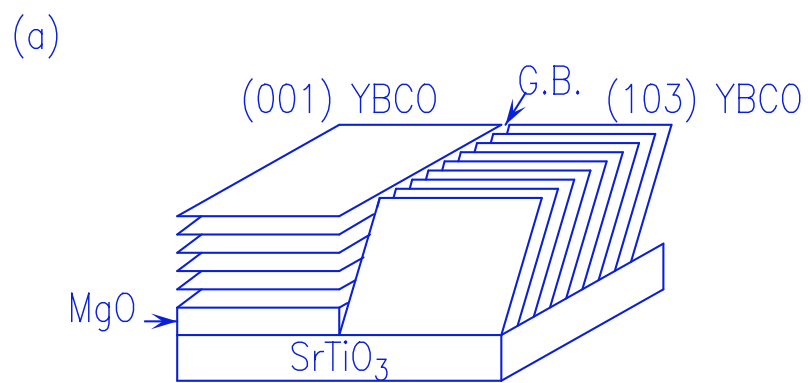
FIG. 4. (a) Scanning SQUID microscope images of a (001)/(103) biepitaxial SQUID, cooled in a field of 3mG, and imaged at $T=60\text{K}$. Also shown are histograms of the frequency of occurrence of SQUID sensor fluxes above areas (outlined by dashed lines) in the (001) (b) and (103) (c) regions of the sample. The (001) region shows a much broader distribution due to spontaneous magnetization, but both regions show diamagnetic shielding.

SSM

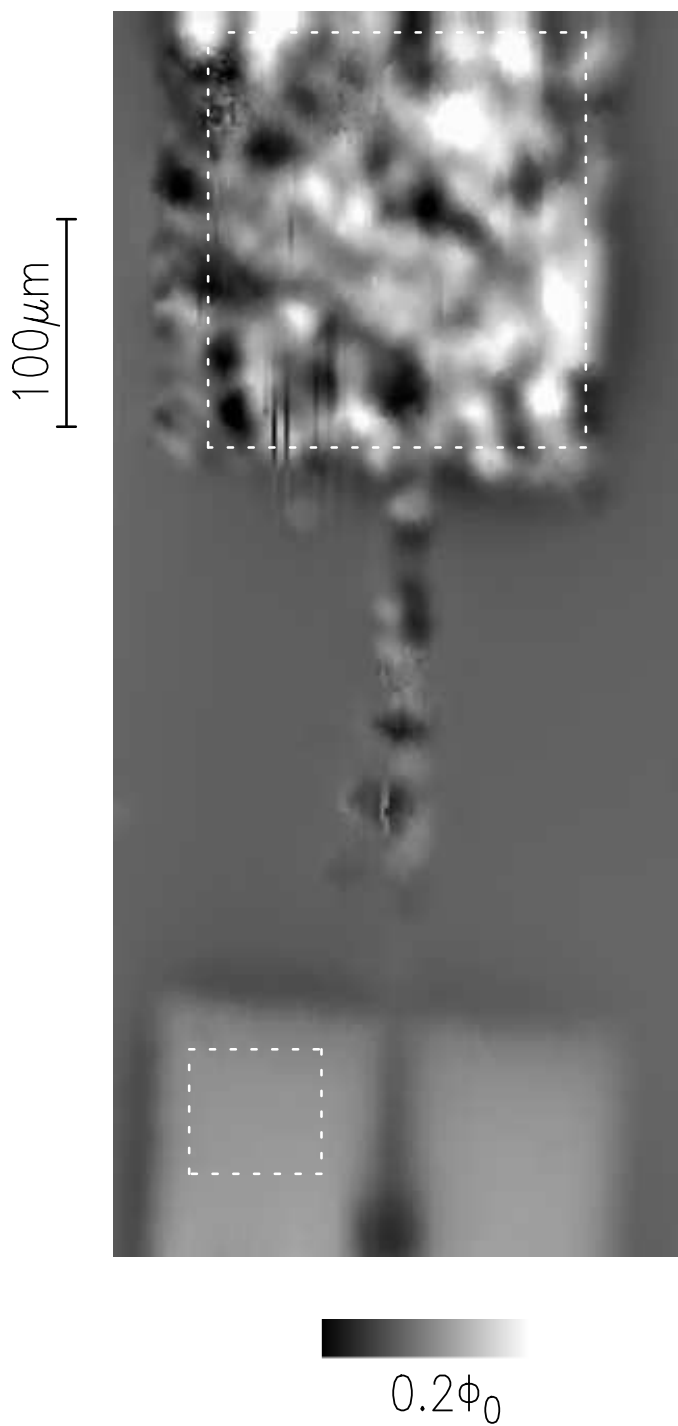


SEM

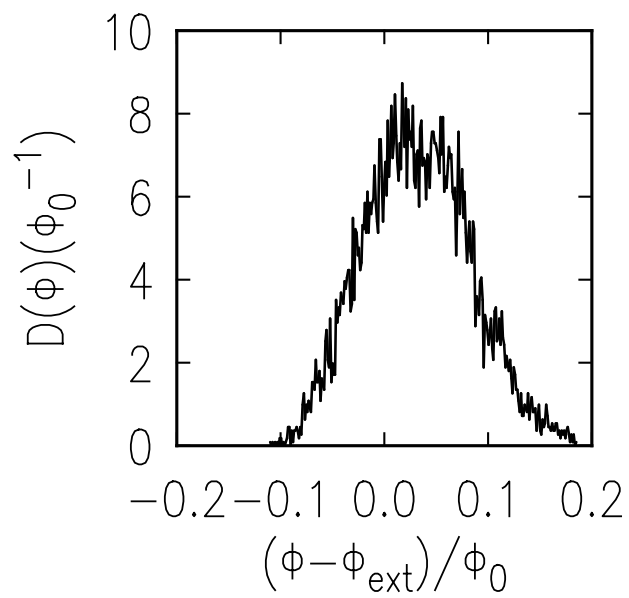




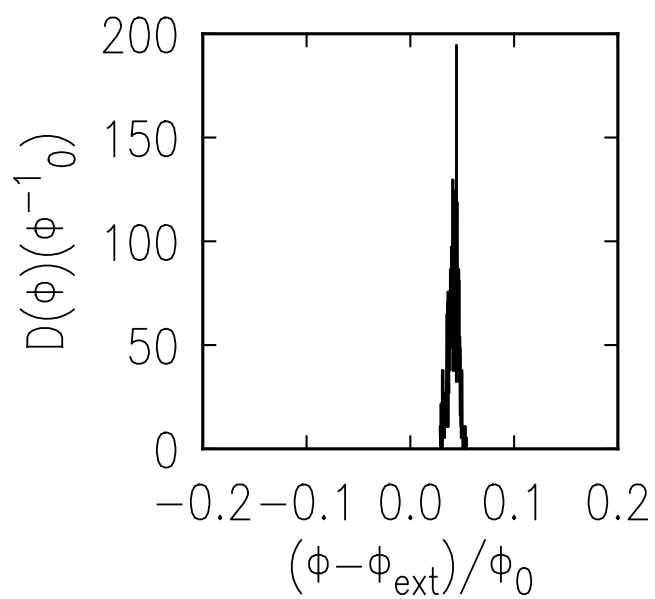
(a)



(b)



(c)

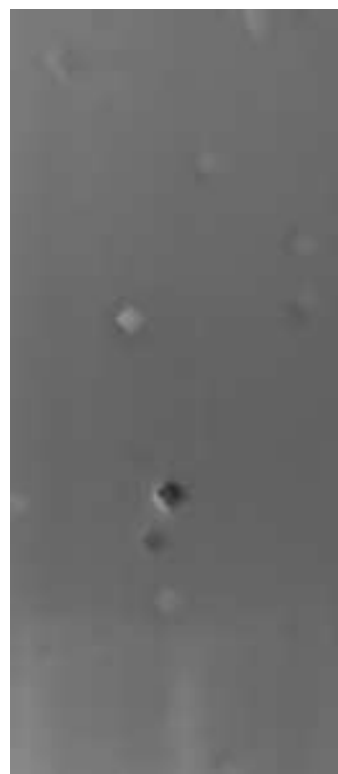
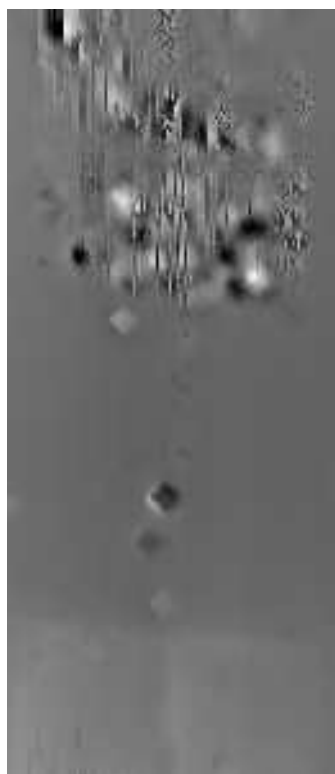


60 K

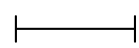
70 K

75 K

80 K



$0.11\phi_0$



$100\mu\text{m}$